Reactions of Coordinated Molecules. 35. Carbon-Carbon Bond Formation between Adjacent Acyl Ligands in (Metalla-β-diketonato)difluoroboron Complexes of Iron, Manganese, and Rhenium

P. Galen Lenhert,[1a] C. M. Lukehart,*[1b] and K. Srinivasan[1b]

Contribution from the Departments of Chemistry and Physics and Astronomy, Vanderbilt University, Nashville, Tennessee 37235. *Received May 9, 1983*

Abstract: When ferra-, mangana-, or rhena-β-diketonate complexes of the type $L_nM(CH_3CO)(RCO)BF_2$ are treated with KH or tetramethylpiperidine, a proton is removed from the acetyl ligand to give anionic η^3-allyl complexes of the type $\{L_nM[\eta^3\text{-}CH_2COCO(R)BF_2]\}^-$. The metal fragments, L_nM, include $(\eta\text{-}C_5H_5)(OC)Fe$, *cis*-$(OC)_4Mn$, and *cis*-$(OC)_4Re$, and R is methyl or isopropyl. For the Re complex with R being isopropyl, the deprotonation occurs either at the acetyl or isobutyryl ligand. Pyridine is basic enough to effect deprotonation, also. Formation of the η^3-allyl complexes occurs by an interligand, C–C bond formation between the original two acyl carbon donor atoms of the metalla-β-diketonate complexes. An X-ray structure of PPN $\{cis\text{-}(OC)_4Mn[\eta^3\text{-}CH_2COCO(i\text{-}Pr)BF_2]\}$ is reported: $P2_1/c$ with a = 14.573 (4) Å, b = 17.472 (4) Å, c = 20.175 (5) Å, β = 123.03 (2)°, V = 4307 Å^3, and Z = 4. The general nature of this interligand, C–C bond formation is now clearly established.

We reported recently an intramolecular, interligand C–C bond formation reaction that occurs between adjacent acyl ligands, as shown in eq 1.[2] When the (ferra-β-diketonato)difluoroboron

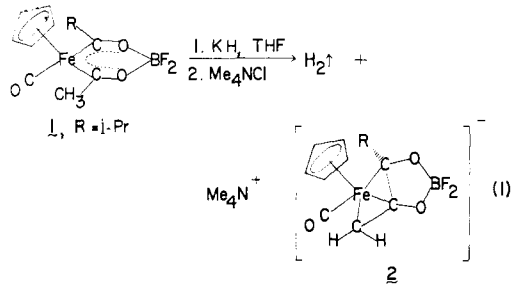

complex **1** is treated with KH, a proton is removed from the methyl substituent of the ferra chelate ring, and complex **2** forms in essentially quantitative yield with concomitant elimination of molecular hydrogen. Complex **2** is an η^3-allyl complex (written in an all-σ representation) as determined by X-ray crystallography.

We can *rationalize* the rearrangement of the α-enolate anion of **1** to **2** by using a single set of Lewis structures, as shown in eq 2. The initial enolate anion of **1** is represented as **3**. Structure

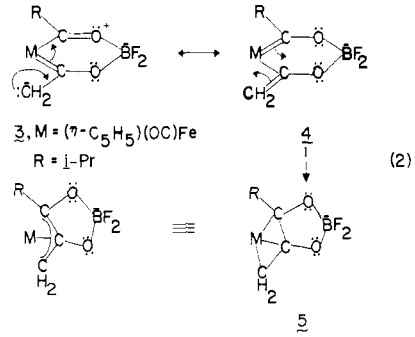

4 is presumably a better description of anion **3**, because the negative charge on the α-carbon atom is stabilized by the metalla chelate ring. Structure **4** contains formally a Fischer-carbenoid ligand and an η^1-alkenyl ligand bonded to the iron atom. Both of these ligand types are known to form stable complexes with cyclopentadienyliron carbonyl moieties. Conversion of **4** to the observed product **5** occurs as a metal-mediated, transannular C–C bond formation. The formal oxidation state of M does not change in going from **1** to **2** (or **5**), nor has a reductive-elimination reaction occurred.

As noted recently by us,[3] if the metalla moiety, M, in **4** is presumed to be isolobal[4,5] to an sp^2-CH group, then in structure **5**, M is isolobal to an sp^3-CH group. Structure **4** is formally a transoid 2-metalla-1,3-butadiene, and **5** is formally a 1-metallabicyclo[1.1.0]butane. The conversion of **4** to **5** represents a *thermally* allowed, concerted $[_\pi 2_a + _\pi 2_s]$ ring closure, in analogy to the pericyclic ring opening of bicyclo[1.1.0] butanes to give *trans, trans*-1,3-butadienes.[6] The transoid metalladiene structure of **4** is imposed on this "intermediate" by the BF_2 chelate ring.

We now report that interligand C–C bond formation between acyl ligands occurs not only in ferra-β-diketonate molecules but also in the isovalent mangana and rhena analogues. An X-ray structure of a mangana-coupled product reveals a structural distortion of the $Mn(CO)_4$ group which is opposite to the distortion observed in mangana-β-diketonato complexes but which is in the correct direction for an $Mn(CO)_4$ group acting as an isolobal analogue to an sp^3-CH group.[7] Furthermore, because the acyl carbon donor atoms of **3** (or **4**) undergo a formal reductive coupling (as M is oxidized by one electron and then subsequently reduced by one electron when the new M–C bond is formed), these reactions extend the known examples of metal-mediated reductive coupling of terminal isocyanide and carbonyl ligands[8-10] to include now acyl ligands.

Experimental Section

All reactions and other manipulations were performed under dry, prepurified nitrogen. Tetrahydrofuran (THF) was dried over Na/K alloy

(1) (a) Department of Physics and Astronomy. (b) Department of Chemistry.
(2) Lukehart, C. M.; Srinivasan, K. *J. Am. Chem. Soc.* **1981**, *103*, 4166-4170.
(3) Lukehart, C. M.; Srinivasan, K. *Organometallics* **1982**, *1*, 1247-1249.
(4) Elian, M.; Chen, M. M. L.; Mingos, D. M. P.; Hoffmann, R. *Inorg. Chem.* **1976**, *15*, 1148-1155.
(5) Hoffmann, R. *Angew. Chem., Int. Ed. Engl.* **1982**, *21*, 711-724.
(6) Closs, G. L.; Pfeffer, P. E. *J. Am. Chem Soc.* **1968**, *90*, 2452-2453.
(7) Elian, M.; Hoffmann, R. *Inorg. Chem.* **1975**, *14*, 1058-1076.
(8) Lam, C. T.; Corfield, P. W. R.; Lippard, S. J. *J. Am. Chem. Soc.* **1977**, *99*, 617-618.
(9) Berry, D. H.; Bercaw, J. E.; Jircitano, A. J.; Mertes, K. B. *J. Am. Chem. Soc.* **1982**, *104*, 4712-4715.
(10) Hoffmann, R.; Wilker, C. N.; Lippard, S. J.; Templeton, J. L.; Brower, D. C. *J. Am. Chem. Soc.* **1983**, *105*, 146-147, and references therein.

0002-7863/84/1506-0124$01.50/0

with added benzophenone. Methylene chloride and acetone-d_6 were dried over P_2O_5.

Infrared (IR) spectra were recorded on a Perkin-Elmer 727 spectrometer as methylene chloride solutions in 0.10-mm sodium chloride cavity cells with the solvent as a reference and a polystyrene film as a calibration standard. ^1H NMR spectra were obtained on a JEOL MH-100 NMR spectrometer as either acetone-d_6 or $CDCl_3$ solutions with Me_4Si as an internal reference. ^{13}C NMR spectra were recorded on a JEOL FX 90Q FT NMR spectrometer operating at a frequency of 22.5 MHz at 36 °C. The ^2H signal of the solvent was used as a locking frequency, and a pulse width of 6 μs was used. A repetition rate of 1.7 s was employed to collect ca. 9000 pulses/spectrum. Preliminary spectra were proton decoupled by using a 1000-Hz bandwidth decoupling frequency. Peak assignments and exact C–H coupling constants were obtained by gated decoupling. Samples consisted to ca. 35 mg of complex and 0.5 mg of $Cr(acac)_3$ dissolved in ca. 0.4 mL of solvent with Me_4Si as an internal reference. Microanalysis was performed by Galbraith Laboratories, Inc., Knoxville, TN.

The complexes $(\eta\text{-}C_5H_5)(OC)Fe(CH_3CO)_2BF_2$ (**6**), *cis*-$(OC)_4Mn(CH_3CO)_2BF_2$ (**7**), *cis*-$(OC)_4Re(CH_3CO)_2BF_2$ (**9**), and *cis*-$(OC)_4Re(i\text{-}PrCO)(CH_3CO)BF_2$ (**10**) were prepared by literature methods.[11]

Preparation of *cis*-$(OC)_4Mn(i\text{-}PrCO)(CH_3CO)BF_2$ (8). To a stirred solution of 2.44 g (9.2 mmol) of *i*-PrC(O)Mn(CO)$_5$ in 175 mL of ether at −78 °C was added dropwise 6.13 mL of a 1.5 M solution of methyllithium in ether over a 5-min period. After the solution was stirred at −50 °C for 30 min, the solvent was removed at −10 °C at reduced pressure. The reaction residue was suspended to 150 mL of CH_2Cl_2 and then was cooled to −78 °C. Gaseous BF_3 was bubbled through this suspension at a moderately slow rate for 3 min. After the reaction mixture was stirred at −78 °C for 45 min and then at 0 °C for 2 h, the solvent and excess BF_3 were removed at reduced pressure. The reaction residue was extracted with 90 mL of toluene. The extracted solution was filtered, and the solvent was removed at reduced pressure to give a crude product. Crystallization from ether solution at −20 °C afforded 2.10 g (70%) of **8** as yellow needles: mp 104–105 °C IR (CH_2Cl_2) ν(CO) 2085 (m), 2025 (m), 2005 (vs), 1993 (s) cm^{-1}; ^1H NMR ($CDCl_3$) δ 1.06 (d, 6, Me_2HC, J = 6.5 Hz), 3.10 (s, 3, CH_3CO), 4.00 (heptet, 1, CH, J = 6.5 Hz); ^{13}C NMR ($CDCl_3$) δ 17.8 (q, Me_2CH, J = 129 Hz), 51.2 (q, $MeCO$, J = 129 Hz), 61.5 (d, CH, J = 132 Hz), 206.8 (s, CO equatorial), 207.3 (s, CO equatorial), 213.7 (br s, 2 CO axial), 341.1 (s, Me*CO*), 347.5 (s, *i*-Pr*CO*). Anal. Calcd for $C_{10}H_{10}O_6BF_2Mn$: C, 36.39; H, 3.04. Found: C, 36.39; H, 3.19.

Preparation of $Me_4N\{(\eta\text{-}C_5H_5)(OC)Fe[\eta^3\text{-}CH_2COCO(Me)BF_2]\}$ (11). To a stirred suspension of 0.06 g (1.50 mmol) of KH in 40 mL of THF was added 0.39 g of (1.40 mmol) of **6** at 25 °C. The yellow reaction solution turned red immediately after this addition concomitant with the brisk evolution of hydrogen. The solution was stirred for 20 min, and then the solvent was removed at reduced pressure. To the solid residue were added 4 mL of a saturated solution of Me_4NCl in degassed water and 40 mL of CH_2Cl_2. This mixture was stirred for 20 min. The CH_2Cl_2 layer was dried over 4-Å molecular sieves. Two similar extractions using 40 mL of CH_2Cl_2 were combined and dried. Removal of the solvent at reduced pressure and crystallization of the product from CH_2Cl_2/hexane solution at −20 °C afforded 0.21 g (43%) of **11** as yellow needles: mp 90–110 °C dec; IR (CH_2Cl_2) ν(CO) 1900 (br) cm^{-1}; ^1H NMR (acetone-d_6) δ 0.48 (d, 1, CH_2 anti H, J = 4.5 Hz), 1.27 (s, 3, CH_3), 2.93 (d, 1, CH_2 syn H, J = 4.5 Hz), 3.44 (s, 12, NMe_4^+), 4.32 (s, 5, C_5H_5); ^{13}C NMR (acetone-d_6) δ 15.6 (t, CH_2), ca. 30 (CH_3, obscured by solvent), 56.0 (q of t, NMe_4^+, J_{CN} = 4 Hz), 82.2 (d, C_5H_5), 103.2 (s, *C*Me), 123.1 (s, *C*CH_2), 222.6 (s, CO). Anal. Calcd. for $C_{14}H_{22}NO_3BF_2Fe$: C, 47.08; H, 6.21; N, 3.92. Found: C, 46.60; H, 6.20; N, 4.17.

General Preparation of $Me_4N\{cis\text{-}(OC)_4M[\eta^3\text{-}C)H_2COCO(R)BF_2]\}$ (12–16). To a stirred suspension of 0.05–0.25 g of KH in 40 mL of THF was added a 1 mol equiv of the appropriate (*cis*-tetracarbonylmetalla-β-diketonato)difluoroboron complex at 25 °C. A brisk evolution of hydrogen occurred immediately in all cases, and the extent of reaction was followed by recording IR spectra of the reaction solution at regular intervals. Complexes **7** and **9** reacted completely within 1 h, while complexes **8** and **10** reacted slowly over 8 h. These reactions proceeded more rapidly when the reaction mixtures were exposed to short periods of reduced pressure. Presumably, entrapped hydrogen gas bubbles on the surface of the KH particles inhibited the rate of reaction. After the reaction was complete, the solvent was removed at reduced pressure. The solid residue was treated with 4 mL of a saturated solution of Me_4NCl in degassed water. The product was extracted into 3 × 40 mL portions of CH_2Cl_2, and the combined extracted solutions were dried over 4-Å molecular sieves for 45 min. The CH_2Cl_2 solution was filtered and concentrated to ca. 50 mL, and the pure η^3-allyl complex crystallized from this solution at −20 °C. The detailed characterization of each complex is provided below.

$Me_4N\{cis\text{-}(OC)_4Mn[\eta^3\text{-}CH_2COCO(Me)BF_2]\}$ (12). Light yellow crystals (48%); mp 125–140 °C dec; IR (CH_2Cl_2) ν(CO) 2055 (m), 1955 (s), 1945 (s, sh), 1915 (s) cm^{-1}; ^1H NMR (acetone-d_6) δ 1.53 (d, 1, CH_2 anti H, J = 4.5 Hz), 1.88 (s, 3, CH_3), 2.88 (d, 1, CH_2 syn H, J = 4.5 Hz), 3.42 (s, 12, NMe_4^+); ^{13}C NMR (acetone-d_6) δ 23.2 (t, CH_2, J = 156 Hz), 24.6 (q, CH_3, J = 127 Hz), 56.1 (q, NMe_4^+, J = 144 Hz), 124.8 (s, C allyl), 127.2 (s, C allyl). Anal. Calcd for $C_{12}H_{17}NO_6BF_2Mn$: C, 38.41; H, 4.57; N, 3.73. Found: C, 38.35; H, 4.80; N, 3.88.

$Me_4N\{cis\text{-}(OC)_4Mn[\eta^3\text{-}CH_2COCO(i\text{-}Pr)BF_2]\}$ (13). Light yellow crystals (43%); mp 142–148 °C dec; IR (CH_2Cl_2) ν(CO) 2050 (m), 1955 (s), 1945 (s, sh), 1915 (s) cm^{-1}; ^1H NMR (acetone-d_6) δ 1.12, 1.17, 1.19 (3 maxima, 3, $CHMe_2$), 1.51 (br s, 4 $CHMe_2$), 1.53 (d, 1, CH_2 anti H, J = 6 Hz), 2.95 (d, 1, CH_2 syn H, J = 6 Hz), 3.46 (s, 12, NMe_4^+); ^{13}C NMR (acetone-d_6) δ 22.1 (q, $CHMe_2$, J = 126 Hz), 23.5 (t, CH_2, J = 154 Hz), 25.2 (q, $CHMe_2$, J = 127 Hz), 37.2 (d, $CHMe_2$, J = 132 Hz), 56.1 (q of t, NMe_4^+, J_{C-H} = 144 Hz, J_{C-H} = 4.5 Hz), 127.5 (s, C allyl), 133.7 (s, C allyl). Anal. Calcd for $C_{14}H_{21}NO_6BF_2Mn$: C, 41.73; H, 5.21; N, 3.45. Found: C, 41.72; H, 5.48; N, 3.45.

$PPN\{cis\text{-}(OC)_4Mn[\eta^3\text{-}CH_2COCO(i\text{-}Pr)BF_2]\}$ (14). Light yellow crystals of **14** were obtained by the metathetical exchange of K^+ for PPN^+, bis(triphenylphosphine)nitrogen(1+) ion, uisng $[PPN]BF_4$ followed by crystallization from CH_2Cl_2/hexane solution at −20 °C. The X-ray structure of **14** is reported below.

$Me_4N\{cis\text{-}(OC)_4Re[\eta^3\text{-}CH_2COCO(Me)BF_2]\}$ (15). Pale yellow crystals (43%): mp 135–145 °C dec; IR (CH_2Cl_2) ν(CO) 2065 (m), 1970 (vs), 1955 (s), 1915 (s) cm^{-1}; ^1H NMR (acetone-d_6) δ 1.68 (d, 1, CH_2 anti H, J = 6.3 Hz), 2.13 (s, 3, CH_3), 2.88 (d, 1, CH_2 syn H, J = 6.3 Hz), 3.42 (s, 12, NMe_4^+); ^{13}C NMR (acetone-d_6) δ 12.7 (t, CH_2), 26.3 (q, CH_3), 56.0 (q, NMe^+), 108.1 (s, C allyl), 137.8 (s, C allyl), 189.4 (s, CO), 194.1 (s, CO), 196.5 (br s, 2 CO). Anal. Calcd for $C_{12}H_{17}NO_6BF_2Re$: C, 28.47; H, 3.36; N, 2.77. Found: C, 28.45; H, 3.45; N, 2.75.

$Me_4N\{cis\text{-}(OC)_4Re[\eta^3\text{-}CH_2COCO(i\text{-}Pr)BF_2]\}$ (16). Pale yellow crystals (40%); mp 146–151 °C dec; IR (CH_2Cl_2) ν(CO) 2065 (m), 1970 (vs br), 1915 (s) cm^{-1}; ^1H NMR (acetone-d_6) δ 1.17 (d, 3, $CHMe_2$, J = 5.6 Hz), 1.40 (d, 3, $CHMe_2$, J = 5.6 Hz), 1.46 (heptet, 1, $CHMe_2$, J = 5.6 Hz), 1.69 (d, 1, CH_2 anti H, J = 5.8 Hz), 2.97 (d, 1, CH_2 syn H, J = 5.8 Hz), 3.42(s, 12, NMe_4^+); ^{13}C NMR (acetone-d_6) δ 13.8 (t, CH_2 J = 154 Hz), 23.9 (q, $CHMe_2$, J = 128 Hz), 25.0 (q, $CHMe_2$, J = 128 Hz), 38.4 (d, $CHMe_2$, J = 133 Hz), 56.0 (br q, NMe_4^+, J_{C-H} = 146 Hz), 118.4 (s, *C* *i*-Pr), 139.1 (s, C allyl), 189.2 (s, CO), 194.1 (s, CO), 196.6 (s, CO). Anal. Calcd for $C_{14}H_{21}NO_6BF_2Re$: C, 31.48; H, 3.93; N, 2.62. Found: C, 31.67; H, 3.98; N, 2.63.

Preparation of $[C_9H_{20}N]\{cis\text{-}(OC)_4Mn[\eta^3\text{-}CH_2COCO(Me)BF_2]\}$ (18). To a stirred solution of 0.59 g (2.0 mmol) of complex **7** in 10 mL of CH_2Cl_2 was added dropwise 0.4 mL (2.3 mmol) of tetramethylpiperidine at 25 °C. Within 2 min a yellow solid precipitated, and the reaction mixture was stirred for 20 min to ensure complete reaction. The solvent was removed at reduced pressure, and crystallization of the crude product **18** from 60 mL of CH_2Cl_2 at −20 °C gave 0.61 g (70%) of **18** as a yellow powder: mp 138–152 °C dec; IR (CH_2Cl_2) ν(CO) 2050 (m) 1955 (s) 1950 (s), 1920 (s) cm^{-1}; ^1H NMR (acetone-d_6) δ 1.54 (s, 13, 4 CH_3 + CH_2 anti H), 1.82 (br s, 6, 3 CH_2), 1.89 (s, 3, CH_3), 2.90 (d, 1, CH_2 syn H, J = 5 Hz); ^{13}C NMR (acetone-d_6) δ 16.7 (t, CH_2), 27.6 (q, 4 CH_3), 35.4 (t, 2 CH_2), 58.5 (s, *C*N), 23.2 (t, CH_2), 24.7 (q, CH_3), 123.4 (s, C allyl), 127.6 (s, C allyl). Anal. Calcd for $C_{17}H_{25}O_6NBF_2Mn$: C, 46.10, H, 5.64; N, 3.16. Found: C, 45.96; H, 5.71; N, 3.17.

Preparation of $[C_9H_{20}N]\{cis\text{-}(OC)_4Re[\eta^3\text{-}CMe_2COCO(Me)BF_2]\}$ (21). To a stirred solution of 0.40 g (0.87 mmol) of **10** in 15 mL of CH_2Cl_2 was added 0.15 mL (0.90 mmol) of tetramethylpiperidine at 0 °C. The reaction solution was kept at −20 °C for 12 h during which time a white solid had precipitated. The solvent was removed at reduced pressure, and crystallization of crude **21** from 40 mL of CH_2Cl_2 at −20 °C afforded 0.35 g (67%) of **18** as an off-white solid: mp 136–146 °C dec; IR (CH_2Cl_2) 2055 (m), 1970 (s, sh), 1950 (s), 1920 (s) cm^{-1}; ^1H NMR (acetone-d_6) δ 1.57 (s, 12, 4 CH_3), 1.84 (br s, 6, 3 CH_2), 1.97 (s,

(11) (a) Lukehart, C. M.; Warfield, L. T. *J. Organomet. Chem.* **1980**, *187*, 9–16. (b) Lukehart, C. M.; Warfield, L. T. *Inorg. Chem.* **1978**, *17*, 201–202.

3, anti CH_3), 2.22 (s, 3, CH_3), 2.49 (s, 3, syn CH_3), 6.23 (br s, 2, $R_2NH_2^+$); ^{13}C NMR(THF-d_8) δ 17.0 (t, CH_2, TMP), 27.8 (q, 2 CMe_2, TMP), 28.9 (br q, 2 CH_3 anti), 29.4 (q, CH_3 syn), 35.9 (t, CH_2, TMP), 46.8 (s, CMe_2), 58.1 (t, CMe_2, TMP), 102.3 (s, MeCO), 139.7 (s, C allyl), 189.9 (s, CO), 195.2 (s, CO), 196.5 (br, s, CO). Anal. Calcd for $C_{19}H_{29}O_6NBF_2Re$: C, 46.10; H, 5.64; N, 3.16. Found: C, 45.96; H, 5.71; N, 3.17.

Crystal and Molecular Structure of PPN{*cis*-$(OC)_4Mn[\eta^3$-$CH_2COCO(i\text{-}Pr)BF_2]$} (14). Collection of X-ray Diffraction Data. Precession photographs of a very small crystal showed $2/m$ Laue symmetry with possible systematic abscences of $0k0$ for k odd and $h0l$ for l odd. The preliminary assignment of the space group as $P2_1/c$ was confirmed by subsequent successful refinement of the structure. Cell parameters were determined by least-squares fit of 2θ, ω, and χ diffractometer settings for 14 reflections in the range $26° < 2\theta < 31°$ as measured at both $\pm 2\theta$ with Mo $K\alpha_1$ radiation ($\lambda = 0.70926$ Å). Values for a, b, c, and β, respectively, at 20 °C are 14.573 (4) Å, 17.472 (4) Å, 20.175 (5) Å, and 123.03 (2)°, and the calculated volume of the cell is 4307 Å^3. With $Z = 4$ and a molecular weight of 867.15, the calculated density is 1.337 g cm^{-3}.

Intensity data were collected from a small crystal measuring 0.15 mm × 0.14 mm × 0.04 mm (volume 0.009 mm^3) which was mounted with the large face (100) parallel to the ϕ axis on the four-circle automated diffractometer. The control software for the Picker FACS-I system has been reported previously.[12] All reflections out to 40°, 2θ, in the $\pm h,k,\pm l$ quadrants were measured with step scans across the peak. The radiation was Mo $K\alpha$ from a highly oriented graphite crystal and the step scans consisted of 11 steps per reflection spaced at 0.03° 2θ with each step counted for 20 s. Background was measured above and below each reflection for a total of 200 s. Three monitor reflections showed an intensity decline of approximately 20% during the course of 800 h of X-ray exposure. Absorption corrections were calculated for the 8235 reflections with ORABS[13] using a linear absorption coefficient of 4.22 cm^{-1} and an 8 × 8 × 8 Gaussian grid. The maximum and minimum transmission factors were 0.98 and 0.95. Symmetry equivalent reflections were averaged to give a set of 4025 reflections.

Solution and Refinement. A sharpened, origin-removed Patterson map revealed the Mn–Mn vectors and one set of P–P vectors in the Harker section and Harker line. Several cycles of refinement and difference syntheses led to the location of all non-hydrogen atoms. Least-squares refinement proceeded; with most hydrogen atoms placed and with anisotropic thermal parameters for all non-hydrogen atoms, R remained at 13.2%. A number of small peaks (1–2 e Å^{-3} in height) remained. Eventually a model that accounted for these peaks was constructed. It assumed that two molecular conformations—approximately related by a mirror plane through Mn, C(1), C(3), C(4), C(5), C(8), and B—were present. The disorder model required a major and minor site for C(2), O(2), O(5), C(6), O(6), C(7), F(1), and F(2). In addition, rotational disorder in the isopropyl group required a major and minor site for C(9) and C(10). After fixing the thermal parameters, occupation factors were refined for atoms at the minor sites. The resulting occupation factors were averaged and the result, 0.29, was used for all subsequent calculations. The molecular configuration of the major-site anion is shown in Figure 1, while a figure showing the relation of the major and minor site anions is provided in the supplementary material. Three atoms of the η^3-allyl ligand, C(8), C(5), and B occupy the same position in both orientations. After preliminary refinement with the new model, hydrogen positions were recalculated (a difference synthesis was used as a guide for those attached to methyl carbon atoms). No difficulty was encountered in refining the coordinates of the major and minor site atoms except for the minor site atoms of the isopropyl group, C(9) and C(10), which did not converge and were fixed. Final least-squares refinement was carried out with all refinable parameters included in a single matrix which gave $R = 8.4\%$ for 3270 reflections where $F^2 > \sigma(F^2)$.

Least-squares refinement minimized $\sum w(|F_o| - |F_c|)^2$ where $w = 1/\sigma(F_o)^2$. The variance, σ^2, was based on counting statistics, and it included the usual instability term (4.0% in this case) as described previously.[14] Atomic scattering factors for neutral atoms were those tabulated by Cromer and Mann[15] and the anomalous scattering factors were those given by Cromer and Lieberman.[16] The final weighted R factor, R_w, was 7.3% for $F^2 > \sigma(F^2)$ where $R_w = \{[\sum w(|F_o| - |F_c|)^2]/\sum w|F_o|^2\}^{1/2}$. Corresponding values for R and R_w for $F^2 > 3\sigma(F^2)$ are 6.3% and 6.6%, respectively. The average and maximum shift-to-error ratio for the final refinement cycle were 0.03 and 0.14. The maximum and minimum electron density on the final difference map were +0.37 and −0.37 e Å^{-3} near Mn and P(1). A complete listing of final positional parameters is provided in Table I. The values were used before rounding to calculate the final structure factors. A complete lisitng of thermal parameters, a listing of F_o and F_c values, tabulations of selected bond distances and angles for the minor-site molecule, and least-squares planes data are included in the supplementary material.

Structure factor, electron density, bond distance and angles, and least-squares calculations were performed with the X-RAY 67 programs[17] as implimented and updated on the Vanderbilt DEC 10 computer.

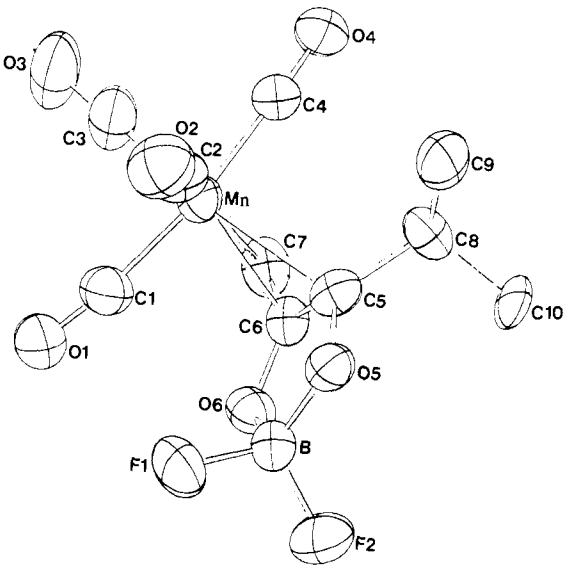

Figure 1. An ORTEP view of the anionic complex of the PPN{*cis*-$(OC)_4Mn[\eta^3$-$CH_2COCO(i\text{-}Pr)BF_2]$} (**14**) molecule of occupation factor 71% showing the atomic numbering scheme (thermal ellipsoids at 30% probability). Hydrogen atoms are not shown.

Results

The general base-induced, interligand C–C bond formation reaction is shown in eq 3. When the ferra-, and mangana-, and

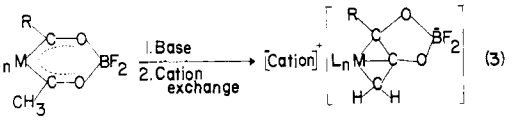

(3)

rhena-β-diketonato complexes, **1** and **6–10**, are treated with Brønsted bases, a proton is removed from a methyl substituent of the metalla-β-diketonate rings, and the η^3-allyl complexes **2**[2] and **11–21** are formed (Table II).

With KH as the Brønsted base, the new complexes **11–16** are isolated as the Me_4N^+ or PPN^+, bis(triphenylphosphine)nitrogen(1+) salts by cation exchange. The X-ray structure of the only PPN^+ salt, **14**, is discussed below. The Me_4N^+ salts **11–13**, **15**, and **16** are isolated in 40–48% yield as yellow solids of high thermal stability.

With TMP (tetramethylpiperidine) as the Brønsted base, the iron and manganese η^3-allyl complexes **17–19** are formed as the $TMPH^+$ salts. Complex **18** is prepared and isolated (in 70% yield) on a synthetic scale, while complexes **17** and **19** were prepared in NMR-tube reactions.

Reactant complexes **1**, **8**, and **10** contain both methyl and isopropyl substituents on the metalla chelate ring. Upon treatment with base, deprotonation could occur either at the methyl sub-

(12) Lenhert, P. G. *J. Appl. Crystallogr.* **1975**, *8*, 568–570.
(13) Wehe, D. J.; Busing, W. R.; Lenz, H. A. "ORABS, A Fortran Program for Calculating Single-Crystal Absorption Corrections", Report ORNL-TM-229; Oak Ridge National Laboratory: Oak Ridge, TN, 1962.
(14) Miller, P. T.; Lenhert, P. G.; Joesten, M. D. *Inorg. Chem.* **1972**, *11*, 2221–2227.
(15) Cromer, D. T.; Mann, J. B. *Acta Crystallogr., Sect. A* **1968**, *A24*, 321–324.
(16) Cromer, D. T.; Lieberman, D. *J. Chem. Phys.* **1970**, *53*, 1891–1898.
(17) Stewart, J. M. "X-Ray 67 Program System for X-Ray Crystallography for the Univac 1108, CDC 3600/6600, IBM 360/50, 65, 75, IBM 7094", Technical Report Tr-67-58; Computer Science Center, University of Maryland: College Park, MD, 1967.

Table I. Final Positional Parameters[a] for PPN {*cis*-$(OC)_4Mn[\eta^3$-$CH_2COCO(i$-Pr)$BF_2]$} (**14**)

atom[b]	occupation[c] factor	*x*	*y*	*z*	atom[b]	*x*	*y*	*z*
Mn		0.7325 (2)	0.09586 (8)	0.01944 (9)	C(22)	0.028 (1)	0.4124 (6)	0.3241 (8)
F(1)	0.71	0.6498 (9)	0.3108 (5)	−0.0139 (6)	C(23)	−0.0556 (9)	0.4015 (7)	0.2484 (7)
F(2)	0.71	0.749 (2)	0.3649 (7)	−0.0556 (9)	C(24)	−0.0749 (8)	0.3325 (7)	0.2150 (6)
O(1)		0.7153 (7)	0.2052 (5)	0.1257 (6)	C(25)	−0.0084 (8)	0.2723 (6)	0.2587 (6)
O(2)	0.71	0.4971 (9)	0.1138 (7)	−0.0925 (8)	C(30)	0.0830 (8)	0.1266 (5)	0.3930 (6)
O(3)		0.726 (1)	−0.0179 (6)	0.1239 (8)	C(31)	−0.019 (1)	0.1421 (6)	0.3778 (7)
O(4)		0.7682 (7)	−0.0414 (5)	−0.0510 (5)	C(32)	−0.077 (1)	0.0839 (8)	0.3870 (8)
O(5)	0.71	0.6775 (8)	0.2399 (6)	−0.1005 (6)	C(33)	−0.034 (2)	0.0140 (8)	0.4059 (8)
O(6)	0.71	0.8211 (8)	0.2595 (7)	0.0325 (6)	C(34)	0.068 (2)	−0.0033 (6)	0.4211 (7)
B		0.722 (2)	0.2944 (9)	−0.0377 (9)	C(35)	0.1263 (9)	0.0546 (7)	0.4135 (6)
C(1)		0.723 (1)	0.1669 (7)	0.0823 (8)	C(40)	0.2250 (8)	0.1685 (5)	0.3378 (6)
C(2)	0.71	0.591 (2)	0.1038 (9)	−0.049 (1)	C(41)	0.1691 (8)	0.1217 (6)	0.2751 (6)
C(3)		0.728 (2)	0.0257 (2)	0.0813 (8)	C(42)	0.209 (1)	0.0994 (6)	0.2293 (6)
C(4)		0.7542 (9)	0.0131 (7)	−0.0250 (7)	C(43)	0.310 (2)	0.1284 (7)	0.2503 (8)
C(5)		0.7438 (9)	0.1763 (7)	−0.0710 (7)	C(44)	0.3693 (9)	0.1749 (6)	0.3137 (8)
C(6)	0.71	0.827 (2)	0.187 (1)	0.007 (1)	C(45)	0.3278	0.1970 (5)	0.3596 (6)
C(7)	0.71	0.898 (2)	0.131 (2)	0.062 (9)	C(50)	0.4266 (8)	0.2952 (5)	0.6117 (6)
C(8)		0.7573 (9)	0.1313 (6)	−0.1288 (6)	C(51)	0.4299 (8)	0.3507 (6)	0.5647 (6)
C(9)	0.71	0.641 (2)	0.0965 (1)	−0.1946 (9)	C(52)	0.502 (1)	0.4125 (7)	0.6022 (9)
C(10)	0.71	0.788 (2)	0.1860 (9)	−0.1718 (9)	C(53)	0.567 (1)	0.4184 (7)	0.6828 (9)
F(102)	0.29	0.772 (3)	0.326 (2)	0.036 (2)	C(54)	0.5631 (9)	0.3621 (8)	0.7285 (7)
F(202)	0.29	0.692 (2)	0.360 (2)	−0.088 (2)	C(55)	0.4936 (9)	0.3006 (6)	0.6924 (7)
O(202)	0.29	0.962 (3)	0.120 (2)	0.121 (2)	C(60)	0.2703 (8)	0.1916 (5)	0.6159 (6)
O(502)	0.29	0.793 (3)	0.249 (2)	−0.052 (2)	C(61)	0.1632 (9)	0.2188 (6)	0.5816 (6)
O(602)	0.29	0.626 (2)	0.250 (2)	−0.063 (2)	C(62)	0.1110 (9)	0.2031 (7)	0.6211 (8)
C(202)	0.29	0.877 (3)	0.112 (2)	0.079 (2)	C(63)	0.165 (1)	0.1647 (7)	0.6910 (8)
C(602)	0.29	0.648 (4)	0.184 (3)	−0.083 (3)	C(64)	0.269 (1)	0.1376 (6)	0.7239 (6)
C(702)	0.29	0.572 (6)	0.122 (3)	−0.098 (4)	C(65)	0.3210 (8)	0.1523 (6)	0.6849 (6)
C(902)	0.29	0.878	0.118	−0.096	C(70)	0.4279 (8)	0.1344 (5)	0.5802 (5)
C(1002)	0.29	0.701	0.174	−0.208	C(71)	0.5238 (8)	0.1474 (6)	0.5827 (6)
P(1)		0.1667 (2)	0.2032 (2)	0.3923 (2)	C(72)	0.5902 (8)	0.0866 (7)	0.5906 (6)
P(2)		0.3398 (2)	0.2136 (2)	0.5648 (2)	C(73)	0.563 (1)	0.0140 (6)	0.5966 (6)
N		0.2562 (6)	0.2352 (4)	0.4756 (4)	C(74)	0.468 (1)	0.0001 (6)	0.5931 (6)
C(20)		0.0771 (7)	0.2807 (5)	0.3356 (6)	C(75)	0.3999 (8)	0.0601 (6)	0.5857 (6)
C(21)		0.0957 (8)	0.3513 (7)	0.3694 (6)				

[a] Nonrefined hydrogen atom positions are included in the supplementary Material; *x*, *y*, and *z* are fractional coordinates with estimated standard deviations in parentheses. [b] Atom designations involving three digits refer to the corresponding atom in the molecule of lower occupancy. Carbon atom designations involving two digits are phenyl carbons of the PPN cation. Atom P(1) is bonded to C(20), C(30), and C(40), while atom P(2) is bonded to C(50), C(60), and C(70). [c] Occupation factors are one, unless specified otherwise.

Table II. Reaction Information for Equation 3

L_nM	R	compd	base	cation$^+$	compd
$(C_5H_5)(OC)Fe$	Me	**6**	KH	Me_4N^+	**11**
	i-Pr	**1**	KH	Me_4N^+	**2**
$(OC)_4Mn$	Me	**7**	KH	Me_4N^+	**12**
	i-Pr	**8**	KH	Me_4N^+	**13**
				PPN^+	**14**
$(OC)_4Re$	Me	**9**	KH	Me_4N^+	**15**
	i-Pr	**10**	KH	Me_4N^+	**16**
$(C_5H_5)(OC)Fe$	*i*-Pr	**1**	TMP	$TMPH^+$	**17**
$(OC)_4Mn$	Me	**7**	TMP	$TMPH^+$	**18**
	i-Pr	**8**	TMP	$TMPH^+$	**19**
$(OC)_4Re$	*i*-Pr	**10**	TMP	$TMPH^+$	**20** + **21** (see text)

stituent or at the isopropyl methine carbon atom. Deprotonation at the methyl substituent is preferred kinetically to deprotonation at the methine carbon atom of the isopropyl substituent.[18] All three complexes react with KH to give the methyl-deprotonated η^3-allyl complexes, as shown in eq 3. The ferra-, and mangana-β-diketonato complexes **1** and **8** react also with TMP to give only the methyl-deprotonated η^3-allyl complexes, **17** and **19**. However, when the rhena-β-diketonato complex **10** is treated with TMP in CH_2Cl_2 solution below room temperature on a synthetic scale, the η^3-allyl complex isolated (in 67% yield) corresponds to deprotonation of the isopropyl substituent methine carbon atom to give complex **21** as the $TMPH^+$ salt (^1H NMR data also indicate that **21** is formed in ca. 5% yield from the reaction of **10** with KH).

(18) House, H. O.; Trost, B. M. *J. Org. Chem.* **1965**, *30*, 1341–1347.

Table III. Results for Reaction of **10** with TMP

no. of equiv of TMP	solvent	*T*, °C	product ratio, **21**:**20**
1.2	acetone-d_6	36	1:5
1.2	CD_2Cl_2	36	1:1
1.2	THF	25	1:3
1.5	CH_2Cl_2	20–25	3:1
1.5	CH_2Cl_2	0–15	6:1

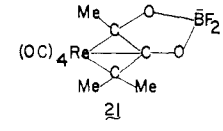

21

When the reaction of **10** with TMP is conducted under various conditions both the "normal" CH_2–allyl product, **20**, and the *gem*-Me_2C–allyl product, **21**, are formed in different relative amounts. These data are summarized in Table III. The product ratio is strongly dependent on temperature and the nature of the solvent. Deprotonation of the isopropyl substituent of **10** by TMP to give **21** becomes more preferred at lower temperature and in an unoxygenated solvent, like CH_2Cl_2. Independent NMR experiments near room temperature reveal that the structural isomers

20 and **21** do not interconvert. These results might be consistent with the formation and rapid equilibration of the two possible enolate anions prior to C–C bond formation. Mechanistic studies that examine this presumption are under way.

Quite surprisingly, complex **7** reacts with pyridine to give **12** (as the pyridinium salt) as revealed by the observation of the η^3-allyl doublet resonances in the ^{1}H NMR spectrum for the syn and anti allylic protons and a singlet resonance for the *anti*-methyl substituent. Therefore, the methyl substituents of these (metalla-β-diketonato) difluoroboron complexes are quite acidic.

IR Spectra. As the neutral (metalla-β-diketonato)difluoroboron complexes are converted into the anionic η^3-complexes, the carbonyl ligand stretching frequencies shift to lower energy and the intraring C=O ·C bands disappear, as expected. For example, the most intense ν_{CO} band of **8** at 2005 cm^{-1} shifts to 1955 cm^{-1} in the allyl product, **13**.

^{1}H NMR Spectra. Several diagnostic changes occur in the ^{1}H NMR spectrum as a (metalla-β-diketonato)difluoroboron complex is converted into the anionic η^3-allyl complex. For the (ferraacetylacetonato)difluoroboron complex, **6**, the singlet resonance at δ 2.88 for the chelate-ring methyl substituents disappears upon formation of the product **11** and gives rise to the syn and anti allylic proton doublet resonances at δ 2.93 and 0.48, respectively, and the singlet resonance at δ 1.27 for the *anti*-methyl substituent.[19] The C_5H_5 singlet of **11** shifts 0.78 ppm to higher field than its position in **6**. This shift is consistent with an increased negative charge density at the iron atom after formation of the η^3-allyl ligand.

Similar spectral changes are observed for the mangana and rhena complexes. For the (metalla-β-diketonato)difluoroboron complexes **7–10**, the chelate ring methyl substituent resonances appear in the range δ 2.90–3.10. Conversion of these complexes to the η^3-allyl products, **12**, **13**, **15**, **16**, and **18**, affords syn and anti allylic proton doublet resonances at average chemical shifts of δ 2.92 and 1.73, respectively. The *anti*-methyl substituent resonances of **12**, **15**, and **18** occur at an average chemical shift of 1.58 δ.

The *anti*-isopropyl substituents of **13** and **16** possess magnetically nonequivalent methyl groups, as expected from the C_1 symmetry of the complexes. These methyls are isochronous in the (metalla-β-diketonato)difluoroboron complexes **8** and **10**. This anisochronism of the isopropyl methyl groups is well resolved in the spectrum of **16** but is less well resolved in the spectrum of **13** due partially to overlapping resonances. The 100-MHz spectrum of **13** at −30 °C reveals a resolved doublet for the anti allylic hydrogen atom due to a temperature dependent chemical shift. The isopropyl methyl resonance at δ 1.51 still overlaps with the methine proton resonance at this temperature. However, the other isopropyl methyl resonance of **13**, which is chemical shift separated and centered at δ 1.17, is more complex than the expected doublet. The reason for the complexity of this band is not obvious. Because the Mn atoms in **13** obeys the effective atomic number rule, an Mn···H–CMe$_2$ interaction, like that observed in 16-electron (η^3-allyl)manganese complexes by Brookhart,[20] is not likely. A dynamic intramolecular motion of the η^3-allyl ligand of **13** is not obvious either. An X-ray structure of the PPN$^+$ salt of this organometallic complex is presented below to provide unambiguous characterization of this complex.

^{13}C NMR Spectra. Several diagnostic changes also occur in the ^{13}C NMR spectra as (metalla-β-diketonato)difluoroboron complexes are converted to η^3-allyl complexes. For the reactant complexes **6–10**, the chelate-ring, methyl substituent resonances appear at an average chemical shift of δ 51.9 (within a range δ 49.3–53.9), and the chelate-ring, acyl-carbon resonances appear at an average chemical shift of δ 329.8 (within a range δ 313.9–347.5 δ).[21,22] For the η^3-allyl products **11–13**, **15**, **16**, and **18**, these carbon atoms comprise the allyl–ligand skeleton. The average resonance of the allyl–CH$_2$ terminal carbon atoms is δ 17.6 (within a range δ 12.7–23.5) and the average resonances for the two quaternary allyl carbon atoms are δ 117.6 (within a range δ 103.2–127.5) and 131.4 (within a range δ 123.1–139.1).

As expected, the low symmetry of the η^3-allyl complexes is evident by the anisochronism of the prochiral methyl groups of the isopropyl substituents. In complexes **13** and **16**, this anisochronism is 3.1 and 1.1 ppm, respectively. The larger anisochronism in **13** might be related to the unusual shapes of the resonances observed for these methyl groups in the ^{1}H NMR spectrum (vide supra).

For the *gem*-Me$_2$C–allyl complex **21**, the allyl carbon resonances appear at δ 46.8, 102.3, and 139.7. Of the three methyl substituents, the two *anti*-methyl carbon resonances appear as a broad quartet at δ 28.9 while the *syn*-methyl carbon resonance appears at δ 29.4.

Table IV. Selected Interatomic Distances (Å) and Angles (deg) with Estimated Standard Deviations for the PPN{*cis*-(OC)$_4$Mn[η^3-CH$_2$COCO(*i*-Pr)BF$_2$]} (**14**) Molecule of Occupation Factor 71%

	Interatomic Distances		
Mn–C(1)	1.83 (2)	C(8)–C(10)	1.51 (3)
Mn–C(2)	1.75 (2)	C(5)–O(5)	1.38 (2)
Mn–C(3)	1.78 (2)	C(6)–O(6)	1.38 (3)
Mn–C(4)	1.82 (2)	B–O(5)	1.43 (2)
Mn–C(5)	2.38 (2)	B–O(6)	1.49 (2)
Mn–C(6)	2.20 (2)	B–F(1)	1.41 (3)
Mn–C(7)	2.16 (2)	B–F(2)	1.40 (3)
C(1)–O(1)	1.16 (2)	N–P(1)	1.564 (6)
C(2)–O(2)	1.17 (2)	N–P(2)	1.572 (7)
C(3)–O(3)	1.16 (3)	P(1)–C(20)	1.795 (8)
C(4)–O(4)	1.16 (2)	P(1)–C(30)	1.82 (2)
C(6)–C(7)	1.42 (3)	P(1)–C(40)	1.82 (2)
C(5)–C(6)	1.39 (2)	P(2)–C(50)	1.795 (9)
C(5)–C(8)	1.51 (2)	P(2)–C(60)	1.84 (2)
C(8)–C(9)	1.60 (2)	P(2)–C(70)	1.80 (1)
	Interatomic Angles		
Mn–C(1)–O(1)	173 (2)	C(7)–Mn–C(3)	112.2 (6)
Mn–C(2)–O(2)	175 (2)	C(7)–Mn–C(4)	88.0 (7)
Mn–C(3)–O(3)	177 (2)	C(8)–C(5)–O(9)	116 (2)
Mn–C(4)–O(4)	177 (2)	C(6)–C(5)–O(5)	111 (2)
C(1)–Mn–C(2)	89.7 (8)	C(5)–O(5)–B	106.4 (9)
C(1)–Mn–C(3)	86.4 (7)	C(6)–O(6)–B	104 (1)
C(1)–Mn–C(4)	168.3 (6)	O(5)–B–O(6)	108 (2)
C(2)–Mn–C(3)	97.4 (8)	O(5)–B–F(1)	112 (2)
C(2)–Mn–C(4)	96.9 (7)	O(6)–B–F(2)	110 (2)
C(3)–Mn–C(4)	83.2 (7)	F(1)–B–F(2)	106 (2)
C(5)–C(6)–C(7)	128 (2)	F(1)–B–O(6)	106 (2)
C(5)–C(8)–C(9)	108 (2)	F(2)–B–O(5)	114 (2)
C(5)–C(8)–C(10)	109 (2)	P(1)–N–P(2)	144.6 (5)
C(9)–C(8)–C(10)	106 (2)	C(20)–P(1)–C(30)	107.5 (5)
C(5)–C(6)–O(6)	110 (2)	C(20)–P(1)–C(40)	106.5 (6)
C(7)–C(6)–O(6)	121 (2)	C(30)–P(1)–C(40)	107.2 (5)
C(8)–C(5)–C(6)	124 (2)	C(50)–P(2)–C(60)	108.4 (6)
C(7)–Mn–C(1)	91.1 (7)	C(50)–P(2)–C(70)	106.8 (5)
C(7)–Mn–C(2)	150.4 (8)	C(60)–P(2)–C(70)	107.6 (5)

Molecular Structure of 14. An ORTEP diagram showing the atomic numbering scheme of the η^3-allyl complex (of higher occupation factor) of the salt **14** is shown in Figure 1. Selected bond distances and angles of this salt are provided in Table IV. The Mn(CO)$_4$ moiety has the expected geometry for a *cis*-M(CO)$_4$L$_2$ complex. The average Mn–C distance to the four terminal CO ligands is 1.80 (2) Å, and the average C–O distance of these C–O ligands is 1.16 (2) Å. The average Mn–C–O angle of the terminal CO ligands is 176 (2)°. The C(1)–Mn–C(4) angle of 168.3 (6)° reveals that the two axial CO ligands are bent slightly

(19) For the product complexes shown in eq 1, the methyl or isopropyl substituent on the terminal allyl carbon atom is required to occupy an anti position because of the stereochemistry of the BO_2F_2 chelate ring.

(20) Brookhart, M.; Lamanna, W.; Humphrey, M. B. *J. Am. Chem. Soc.* **1982**, *104*, 2117–2126.

(21) Darst, K. P.; Lukehart, C. M. *J. Organomet. Chem.* **1978**, *161*, 1–11.

(22) The previously unpublished ^{13}C NMR data for compounds **6** and **7** are included herein: compound **6** (acetone-d_6) δ 49.3 (q, CH_3, J = 127 Hz), 91.0 (d, C_5H_5, J = 178 Hz), 214.3 (s, CO), 329.2 (s, CH_3C); compound **7** ($CDCl_3$) δ 51.2 (q, CH_3, J = 127 Hz), 206.9 (s, CO), 214.0 (s, CO), 341.3 (s, CH_3C).

away from the η^3-allyl ligand. The average value of the OC–Mn–CO angles between *cis*-terminal carbonyl ligands is 90.7 (7)°.

The Mn–allyl outer carbon distances, Mn–C(7) and Mn–C(5), are 2.16 (2) and 2.38 (2) Å, respectively, while the Mn–C(6) inner allyl carbon distance of 2.20 (2) Å has an intermediate value. The perpendicular distance from Mn to the allyl plane defined by [C(5),C(6),C(7)] is 1.75 Å. Relative to the [Mn,C(2),C(3)] plane, the allyl terminus C(7) lies only 0.04 Å from this plane on the lower side toward the boron atom. The other allyl terminus C(5) lies 0.31 Å from this plane to the opposite side, while the middle allyl atom C(6) lies 0.42 Å below this plane on the same side as C(7). The allyl ligand is, therefore, not symmetrically oriented relative to the [Mn,C(2),C(3)] plane.

Within the η^3-allyl ligand, the two allyl C–C distances, C(5)–C(6) and C(6)–C(7), are 1.39 (2) and 1.42 (3) Å, respectively. The sum of the angles about C(5) and C(6) are 351° and 359° which is consistent with nearly planar hybridization, and the average value of the three C(8)–C distances is 1.54 Å. The two allyl carbon–oxygen distances are 1.38 (2) Å. The BO_2F_2 group has essentially pyramidal hybridization about the boron atom [the average value of the six angles centered at B is 109 (2)°], and the average values of the two B–O and two B–F distances are 1.46 (2) Å and 1.41 (3) Å, respectively.

An ORTEP diagram of the minor-site molecule (29% occupation factor) and listings of selected bond distances and angles for this molecule are included in the supplementary material. This molecule exhibits a near enantiomeric disorder in that the allyl carbon C(7) and the C(2) carbonyl ligand are interchanged leaving atoms C(5), C(8), B, Mn, and the C(1), C(3), and C(4) carbonyl ligands common to both the major- and minor-site molecules.

The PPN^+ cation has the usual bent structure.[23] The P–N–P angle is 144.6 (5)°, and the average value of the P–N distances is 1.568 (7) Å. The average values of the P–C distances, the ring C–C distances, and the C–P–C angles are 1.81 (2) Å, 1.38 (2) Å, and 107.3 (6)°, respectively.

Discussion

The η^3-allyl complexes formed according to eq 1 demonstrate that the base-induced, interligand C–C bond formation between the acyl donor atoms of (metalla-β-diketonato)difluoroboron complexes occurs generally for ferra-, mangana-, and rhena-β-diketonate complexes.

Carbonyl ligand C–O stretching vibrational frequencies shift to lower frequency in going from the neutral (metalla-β-diketonato)difluoroboron complexes to the anionic η^3-allyl products due to an apparent increase in electron density at the metal atom. The intrachelate ring C–O stretching bands of the metalla-β-diketonate ligands are not present in the IR spectra of the η^3-allyl complexes.

The ^1H and ^{13}C NMR specta are also consistent with η^3-allyl complex formation. In the ^1H NMR spectra, the observed high-field and low-field doublets assigned to the anti and syn allylic CH_2 protons, respectively, appear at normal frequencies for this general type of ligand.[24] For example, in the iron complex **11** the syn and anti allylic proton doublets appear at δ 2.93 and 0.48. In $(\eta\text{-}C_5H_5)Fe(CO)(\eta^3\text{-}C_3H_5)$, the corresponding resonances appear at δ 2.67 and d 0.68.[25] The close similarity in these frequencies between this neutral complex and the anionic complex **11** supports the location of the formal negative charge of **11** at the boron atom. Similarly, the anionic manganese complex **12** has syn and anti allylic CH_2 resonances at δ 2.88 and 1.53, respectively, while the corresponding resonances of $(\eta^3\text{-}C_3H_5)Mn(CO)_4$ are at δ 2.69 and 1.72.

Complex **21** is unique in this series of η^3-allyl complexes in having both *syn*- and *anti*-methyl substituents on an allyl terminus. These singlet resonances appear at δ 2.49 and 1.97, with the higher-field resonance being assigned to the *anti*-methyl group.[26] This assignment parallels the assignment of *syn*- and *anti*-allylic protons.

In the ^{13}C NMR spectra of the η^3-allyl complexes, the assignment of the allyl CH_2 terminal carbon atom to the highest-field resonance of the three allyl skeletal carbons is unambiguous from the observation of C–H coupling involving the two allylic protons. The assignment of the disubstituted allyic terminal carbon atom to the middle allylic carbon resonance and the lowest-field allylic carbon resonance to the central allylic skeletal atom is made by comparing these chemical shifts to those of less complex η^3-allyl compounds. The ^{13}C NMR spectra of $(\eta^3\text{-}C_3H_5)Mn(CO)_4$ and its 1-ethyl and 1-isopropyl derivatives show average chemical shift values for the CH_2, substituted, and central allylic skeletal carbons of δ 37.0, 75.6, and 91.9, respectively.[27] NMR data for such highly and unusually substituted η^3-allyl complexes like those reported here are not available.

The chelate ring involving coordination to the BF_2 moiety requires that the terminal methyl or isopropyl groups of complexes **11–13**, **15**, **16**, and **18** (for which spectral data are provided) lie in anti positions. In complex **21**, both *syn*- and *anti*-methyl substituents are present on the same allyl terminal carbon atom. By comparison to the spectral data of the above CH_2–allyl complexes, the methyl carbon resonance of **21** at δ 29.4 is assigned to the *syn*-methyl substituent. The ^{13}C NMR spectra of $(Meall)Fe(CO)_4^+$ (Meall = methylallyl) complexes also reveal that the *anti*-methyl substituent resonances appear at higher field than do the resonances of *syn*-methyl substituents.[28] This pattern is consistent with the observed order of the syn- and anti allylic proton resonances. Apparently, ^{13}C NMR data for model $(all)Re(CO)_4$ complexes are not available.[29]

The X-ray structure of **14** confirms unambiguously that the reaction shown as eq 1 affords a η^3-allyl complex from a (mangana-β-diketonato)difluoroboron complex. Molecular structure determinations of complexes **2** and **14** indicate that eq 2 is a general route for effecting C–C bond formation between the acyl carbon donor atoms of metalla-β-diketonate complexes.

The dihedral angle between the allyl carbon plane [C(5),C(6),C(7)] and the molecular "equatorial" plane [Mn,C(2),C(3)] of 115° indicates a slight tilting of the allyl plane from a perpendicular position relative to the "principal" Mn coordination plane. This tilting of the allyl plane is usually observed. In $(\eta^3\text{-}C_3H_5)Mn(CO)_2[P(OMe)_3]_2$, **22**, the corresponding dihedral angle is 109°.[30]

The Mn–C(7), CH_2 outer carbon, and Mn–C(6), center carbon, distances of 2.16 (2) and 2.20 (2) Å, respectively, are essentially equivalent, but the Mn–C(5), disubstituted outer carbon, distance of 2.38 (2) Å is significantly longer. This trend is observed in the analogous iron complex **2** where the corresponding Fe–C(allyl) distances are 2.085 (5), 2.095 (4), and 2.186 (4) Å, respectively. A longer M–C distance to the outer, (oxy)(alkyl)-substituted allyl carbon atom appears to be common to this type of η^3-allyl ligand. The range of Mn–C(allyl) distances in the $\eta^3\text{-}C_3H_5$ complex **22** is 2.11 (2)–2.23 (2) Å. The bond distances and angles within the η^3-allyl ligand of **14** are consistent with those found for complex **2** and for η^3-allyl ligands, in general.[31]

As discussed previously,[3] the molecular structures of tetracarbonyl mangana- and rhena-β-diketonate complexes reveal a significant tilting of the two axial CO ligands *toward* the metalla chelate ring. This structural distortion is consistent with these metal fragments acting as formal metalla analogues to an sp^2-CH group.[32] Conversion of metalla-β-diketonate complexes into

(23) (a) Ruff, J. K.; Schlientz, W. J. *Inorg. Synth.* **1974**, *15*, 84–90. (b) Goldfield, S. A.; Raymond, K. N. *Inorg. Chem.* **1974**, *13*, 770–775. (c) Ginsburg, R. E.; Berg, J. M.; Rothrock, R. K.; Collman, J. P.; Hodgson, K. O.; Dahl, L. F. *J. Am. Chem. Soc.* **1979**, *101*, 7218–7231.

(24) Green, M. L. H.; Nagy, P. L. I. *Adv. Organomet. Chem.* **1964**, *2*, 325–363.

(25) Green, M. L. H.; Nagy, P. L. I. *J. Chem. Soc.* **1963**, 189–197.

(26) McClellan, W. R.; Hoehn, H. H.; Cripps, H. N.; Muetterties, E. L.; Howk, B. W. *J. Am. Chem. Soc.* **1961**, *83*, 1601–1607.

(27) Oudeman, A.; Sorensen, T. S. *J. Organomet. Chem.* **1978**, *156*, 259–264.

(28) Gibson, D. H.; Ong, T.-S. *J. Organomet. Chem.* **1978**, *155*, 221–228.

(29) Mann, B. E.; Taylor, B. F. "^{13}C NMR Data for Organometallic Compounds"; Academic Press: New York, 1981.

(30) Brisdon, B. J.; Edwards, D. A.; White, J. W.; Drew, M. G. B. *J. Chem. Soc., Dalton Trans.* **1980**, 2129–2137.

(31) Clarke, H. L. *J. Organomet. Chem.* **1974**, *80*, 155–173.

η^3-allylic complexes then corresponds to a conversion of the metalla fragment into a formal analogue to an sp^3-CH group. Hoffmann has calculated that such an $Mn(CO)_4$ group should have a slight square-pyramidal distortion,[7] where the two axial CO ligands are tilted *away* from the η^3-allyl ligand. In complex **14**, the two axial CO ligands are tilted away from the η^3-allyl ligand [the C(1)-Mn-C(4) angle is 168.3 (6)°]. If this distortion is caused by primarily electronic factors, then the formal description of these η^3-allyl complexes, like **5** as 1-metallabicyclo[1.1.0]butanes becomes more accurate.[33]

(32) For a qualitative description of bonding within metalla-β-diketonate complexes see: Lukehart, C. M.; Torrence, G. P. *Inorg. Chim. Acta* **1977**, *22*, 131-134.

(33) We do not wish to imply that our results prove that a pericyclic mechanism is correct. In ref 2, we also presented a mechanism involving electrophilic attack by a positively charged acyl carbon atom on the π-electron pair of an adjacent metal-carbon multiple bond with a concomitant reduction of the metal atom. A referee has suggested the inclusion of a "simple vinyl migration to the carbene in order to form the allyl." This mechanism is essentially the same as our **4** to **5** conversion where the electron pairs are moved in a reversed direction.

Acknowledgment. C.M.L. thanks the National Science Foundation (Grant No. CHE-8106140), the donors of the Petroleum Research Fund, administered by the American Chemical Society, and the University Research Council of Vanderbilt University for support of this research. C.M.L. also acknowledges support from the Alfred P, Sloan Foundation as a Research Fellow. P.G.L. acknowledges support from NIH BRSG (Grant No. RR 07089-13).

Registry No. 6, 73426-85-4; **7**, 73426-87-6; **8**, 87842-20-4; **9**, 67619-57-2; **10**, 69090-82-0; **11**, 87842-22-6; **12**, 87842-24-8; **13**, 87842-26-0; **14**, 87842-27-1; **15**, 87842-29-3; **16**, 87842-31-7; **18**, 87861-46-9; **21**, 87869-34-9; *i*-PrC(O)Mn(CO)$_5$, 15022-36-3; BF_3, 7637-07-2.

Supplementary Material Available: A complete listing of final positional and thermal parameters (including hydrogen atoms), final observed and calculated structure factors, selected bond distances and angles (including a labeled ORTEP diagram) of the anion of **14** having a 29% occupation factor, a labeled ORTEP diagram of the PPN cation, and selected least-squares planes data for **14** (30 pages). Ordering information is given on any current masthead page.

The E2 Transition State: Elimination Reactions of 2-(2,4-Dinitrophenyl)ethyl Halides

Joseph R. Gandler* and Takako Yokoyama

Contribution from the Department of Chemistry, California State University, Fresno, California 93740. *Received June 27, 1983*

Abstract: The base-catalyzed elimination reactions of 2-(2,4-dinitrophenyl)ethyl halides in aqueous solution have been investigated. The relative rate constants for the hydroxide ion catalyzed reactions of the fluoride, chloride, bromide, and iodide are 1:2:9:14, respectively, and there is no hydrogen-deuterium exchange into either the fluoride or chloride substrates when the reactions are run in deuterium oxide with deuteroxide ion as the base catalyst. The reactions are general-base catalyzed with Brønsted β values increasing from 0.42 for the iodide to 0.54 for the fluoride, but decreasing as the β-phenyl substituent is made more electron withdrawing in the series 2-(*p*-nitrophenyl)ethyl bromide (0.61) and 2-(2,4-dinitrophenyl)ethyl bromide (0.46). These results are consistent with an E2 mechanism for these substrates and a reaction coordinate that has a major proton transfer component, as described on More O'Ferrall-Jencks energy surfaces. The decrease in β values as the β-phenyl substituent is made more electron withdrawing reverses previously reported trends of increasing β values in the series 2-phenylethyl bromide (0.51) and 2-(*p*-nitrophenyl)ethyl bromide (0.61). This inversion in the trend of β values means that substrate selectivity undergoes an inversion with increasing substrate reactivity; it is consistent with a clockwise rotation of the E2 reaction coordinate, from one with a major diagonal component for 2-phenylethyl halides to one with a major proton transfer component for the nitro-activated derivatives.

2-Arylethyl derivatives have played a central role in studies of olefin-forming β-elimination reactions and in understanding the relationship between the structure of the E2 transition state and changes in reactant and catalyst structure and reaction conditions.[1,2] Results from these studies indicate that as the β-phenyl substituent is made more electron withdrawing the extent of proton transfer to the base catalyst increases for substrates with good leaving groups, such as halide ions,[3,4] but decreases for substrates with poorer leaving groups, such as ammonium ions.[1,2,5-7] Based on these and many other results, including Hammett ρ values which are larger for ammonium ion than halide ion substrates,[1,2] a mapping out of the E2 transition state for these reactions on More O'Ferrall-Jencks energy surfaces[8,9] has been made. For 2-arylethyl halides the results are consistent with a "central" transition state and a reaction coordinate with a large diagonal component.[5,7] For (2-arylethyl)ammonium ions, however, a transition state is suggested with more carbanion character and a reaction coordinate that has a major component of proton transfer.[5,7,10] If this change in behavior is a result of a shift to the E1cB borderline for the ammonium ion substrates,[5,7] then a similar change in behavior should be observed for a series of

(1) Saunders, W. H., Jr.; Cockerill, A. F. "Mechanisms of Elimination Reactions"; Wiley: New York, 1973; Chapter 2.
(2) More O'Ferrall, R. A. In "The Chemistry of the Carbon-Halogen Bond"; Patai, S., Ed.: Wiley-Interscience: New York 1973; Part 2.
(3) Gandler, J. R; Jencks, W. P. *J. Am. Chem. Soc.* **1982**, *104*, 1937.
(4) Hudson, R. F.; Klopman, G. J. *J. Chem. Soc.* **1964**, 5.
(5) Bourns, A. J.; Smith, P. J. *Can. J. Chem.* **1974**, *52*, 749.
(6) Miller, D. J.; Saunders, W. H., Jr. *J. Org. Chem.* **1981**, *46*, 4247.
(7) Winey, D. A.; Thornton, E. R. *J. Am. Chem. Soc.* **1975**, *97*, 3102.
(8) More O'Ferrall, R. A. *J. Chem. Soc.* **1970**, 274.
(9) Jencks, W. P. *Chem. Rev.* **1972**, *72*, 705.
(10) Lewis, D. E.; Sims, L. B.; Yamataka, H.; McKenna, J. *J. Am. Chem. Soc.* **1980**, *102*, 7411.

0002-7863/84/1506-0130$01.50/0